Nanoscale

RSC Publishing

PAPER

View Article Online
View Journal | View Issue

Cite this: *Nanoscale*, 2013, **5**, 4870

Cytotoxicity of surface-functionalized silicon and germanium nanoparticles: the dominant role of surface charges†

Sourav Bhattacharjee,[ab] Ivonne M. C. M. Rietjens,[b] Mani P. Singh,[c] Tonya M. Atkins,[c] Tapas K. Purkait,[d] Zejing Xu,[d] Sarah Regli,[e] Amber Shukaliak,[e] Rhett J. Clark,[e] Brian S. Mitchell,[f] Gerrit M. Alink,[b] Antonius T. M. Marcelis,[a] Mark J. Fink,[d] Jonathan G. C. Veinot,[e] Susan M. Kauzlarich[c] and Han Zuilhof*[a]

Although it is frequently hypothesized that surface (like surface charge) and physical characteristics (like particle size) play important roles in cellular interactions of nanoparticles (NPs), a systematic study probing this issue is missing. Hence, a comparative cytotoxicity study, quantifying nine different cellular endpoints, was performed with a broad series of monodisperse, well characterized silicon (Si) and germanium (Ge) NPs with various surface functionalizations. Human colonic adenocarcinoma Caco-2 and rat alveolar macrophage NR8383 cells were used to clarify the toxicity of this series of NPs. The surface coatings on the NPs appeared to dominate the cytotoxicity: the cationic NPs exhibited cytotoxicity, whereas the carboxylic acid-terminated and hydrophilic PEG- or dextran-terminated NPs did not. Within the cationic Si NPs, smaller Si NPs were more toxic than bigger ones. Manganese-doped (1% Mn) Si NPs did not show any added toxicity, which favors their further development for bioimaging. Iron-doped (1% Fe) Si NPs showed some added toxicity, which may be due to the leaching of Fe^{3+} ions from the core. A silica coating seemed to impart toxicity, in line with the reported toxicity of silica. Intracellular mitochondria seem to be the target for the toxic NPs since a dose-, surface charge- and size-dependent imbalance of the mitochondrial membrane potential was observed. Such an imbalance led to a series of other cellular events for cationic NPs, like decreased mitochondrial membrane potential ($\Delta\Psi_m$) and ATP production, induction of ROS generation, increased cytoplasmic Ca^{2+} content, production of TNF-α and enhanced caspase-3 activity. Taken together, the results explain the toxicity of Si NPs/Ge NPs largely by their surface characteristics, provide insight into the mode of action underlying the observed cytotoxicity, and give directions on synthesizing biocompatible Si and Ge NPs, as this is crucial for bioimaging and other applications in for example the field of medicine.

Received 24th December 2012
Accepted 11th March 2013

DOI: 10.1039/c3nr34266b

www.rsc.org/nanoscale

Introduction

Nanoparticles (NPs), with their unconventional properties[1] and ability to interact with a wide variety of biomolecules, have the potential to revolutionize the medical field, including diagnostics and therapeutics.[2,3] Unfortunately, often the applicabilities of different NPs are hampered by their toxicity.[4,5] Hence, there is a rapidly growing interest in understanding the toxicity of such NPs in more detail, with the aim to control and minimize their toxicity.

Semiconductor quantum dots (SCQDs), like silicon NPs (Si NPs) or germanium NPs (Ge NPs), have recently received significant attention because they can be made into multipotent and biocompatible NPs.[6,7] Si or Ge NPs can be used as vehicles for drug delivery,[8,9] but perhaps the most exciting application of SCQDs can be foreseen in the field of bioimaging.[10,11] The Si NPs or Ge NPs, due to their very small sizes (<5 nm) and intrinsic fluorescence, enjoy an edge over other NPs (like polymer NPs/PNPs[12] and carbon NPs[13]) that need to be functionalized to be fluorescent.

The potential to provide intrinsically non-toxic NPs also makes Si and Ge NPs highly interesting systems. In biological systems the Si NPs may possibly degrade to silicates, although

[a]*Laboratory of Organic Chemistry, Wageningen University, Dreijenplein 8, 6703 HB Wageningen, The Netherlands*

[b]*Division of Toxicology, Wageningen University, Tuinlaan 5, 6703 HE Wageningen, The Netherlands*

[c]*Department of Chemistry, University of California, One Shields Avenue, California 95616, USA*

[d]*Department of Chemistry, Tulane University, New Orleans, Louisiana 70118, USA*

[e]*Department of Chemistry, University of Alberta, Edmonton, Alberta T6G 2G2, Canada*

[f]*Department of Chemical and Biomolecular Engineering, Tulane University, New Orleans, Louisiana 70118, USA*

† Electronic supplementary information (ESI) available: Synthesis and characterization of Si_M-C_3-NH_2 and Si_M-C_3-NH_2-Dex (M = 0, Mn, Fe). See DOI: 10.1039/c3nr34266b

the alkyl surface groups have been reported to retard such breakdown especially in the case of porous Si NPs.[14] For example, in human beings, Si is converted to *orthosilicic acid*/$Si(OH)_4$ and is excreted in the urine.[15,16] Moreover, since they can be synthesized with diameters <5 nm, the sizes of Si NPs and Ge NPs are often below the size threshold for renal clearance of NPs (<5.5 nm) enabling elimination.[17] In addition, unlike the popular but intrinsically toxic Cd-based bioimaging agents, such as CdSe/ZnS quantum dots (QDs),[15] Si and Ge are mostly non-toxic. In line with this, it has been reported for a set of well-characterized, monodisperse (size 1.6 ± 0.2 nm) and fluorescent Si NPs[18,19] that Si NPs may display toxicity or non-toxicity, against human colonic adenocarcinoma Caco-2 and rat alveolar macrophage NR8383 cells, depending on their surface functionalization (Si-C_3H_6-NH_3^+, Si-C_4H_8-N_3 and Si-$C_{11}H_{22}$-COO^-)[10,18,20,21] although many other variations of synthesis of Si NPs exist.[22–33] It was found that cationic Si NP-NH_3^+ were toxic,[34] while the anionic Si NP-COO^- displayed no discernible toxicity in two different toxicity tests (MTT and BrdU).[21]

It has been proposed that the surface properties of NPs determine their interactions with biological systems,[35–37] although little data based on systematic investigations are available. Fortunately, a wide array of synthetic methods has become available for the preparation of surface-functionalized Si and Ge NPs.[38,39] Therefore, a comparative study is now possible, in which the toxicity of the different Si NPs and Ge NPs can be determined with respect to their surface characteristics. This can help gain insight into how surface factors of these NPs can influence the toxicity, although *n*-alkyl terminated uncharged and water-insoluble Si NPs were also reported to show adequate cellular uptake without causing toxicity.[40] To obtain a generally applicable hypothesis, we therefore performed a systematic investigation in which a large series of water-soluble Si NPs and Ge NPs with different properties (sizes, synthetic origin and surface functionalities) were tested for their possible adverse cellular effects.

Rat alveolar macrophage NR8383 and human colonic adenocarcinoma Caco-2 cells provide two adequate *in vitro* testing models for the Si NPs and Ge NPs. The NR8383 lung cells, being macrophages, act as the first line of defense against air-borne foreign pathogens and a toxic effect imparted on them by the NPs can give an idea on how the NPs can influence the innate immune system. Similarly, eyeing the increasing number of food-based applications of different NPs (like silica NPs), Caco-2 cells, being a human colonic cell line, can be an excellent model to test cytotoxicity and extrapolate the data to *in vivo* situations. Due to the ample reported data on the toxicity of NPs on these two cell lines,[12,20,41] a systematic and comparative toxicity testing with a mechanistic perspective can be performed. It is yet not fully clear what might be the mechanism of cytotoxicity for NPs. Although oxidative stress had been recognized as a mechanism,[42,43] some recent reports counter this view and identified intracellular mitochondria as the target and perhaps the starting point of cytotoxicity. Bhattacharjee *et al.*[20] have shown that an isolated mitochondrial fraction from rat liver produced reactive oxygen species (ROS), after being exposed to cationic Si NP-NH_3^+. A recent hypothesis to explain the cytotoxicity of especially the cationic NPs is that the cationic NPs can interfere with the mitochondrial membrane and decouple the electron transport chain (ETC).[44,45] This in turn may lead to an induction of intracellular ROS (like superoxides, peroxides, hydroxyls) production as well as to leaching out of the sequestered calcium from the mitochondria. Interestingly, this can lead to a cytoplasmic calcium overload and initiation of apoptotic cascades. Additionally, a de-coupling of the ETC can cause a decreased cellular ATP production, which may compromise the cellular viability.

The objective of the current paper is thus to investigate the cytotoxicity of a broad series of Si and Ge NPs. To this aim the following features were measured in both the NR8383 and Caco-2 cells after 24 h of exposure to the different Si NPs or Ge NPs (see the quoted references for more detailed expositions of these nine endpoints): (1) cell viability by MTT assay,[46] (2) cell proliferation by BrdU assay,[21] (3) induction of ROS from an isolated rat liver mitochondrial fraction by DCFH-DA assay,[20] (4) change in the mitochondrial membrane potential ($\Delta\Psi_m$),[44] (5) cellular ATP content,[44] (6) cellular ROS production by DCFH-DA assay,[20] (7) cytoplasmic free Ca^{2+} concentration,[47] (8) caspase-3 activity,[44] as a biomarker for apoptotic pathways, and (9) production of TNF-α,[48] as a pro-inflammatory marker. Finally, the obtained data were assembled to propose a series of events that ultimately lead to the toxicity (or lack thereof) of surface-functionalized Si and Ge NPs, and to provide directions to obtain non-toxic Si and Ge NPs.

Materials and methods

Si NPs and Ge NPs

The fully characterized different Si NPs and Ge NPs were obtained as aqueous dispersions. Exposure ranges of the different Si NPs and Ge NPs (concentration 0–100 μg ml^{-1}) were prepared by mixing the aqueous dispersion of NPs with cell culture media (F12-K or DMEM).

NR8383 cells

Rat alveolar macrophage (NR8383) cells were obtained from ATCC (Manassas, VA). The NR8383 cells were cultured in 150 cm^2 cell culture flasks with 25 ml F12-K culture medium (Gibco 21127) supplemented with 10% (v/v) heat inactivated fetal calf serum (FCS) in a humidified atmosphere containing 5% CO_2 at 37 °C. The cells were sub-cultured every two weeks. Cells with passage numbers 30–40 were used.

Caco-2 cells

The Caco-2 cells were obtained from ATCC (Rockville, MD) and were cultured in DMEM medium (Gibco), fortified with 10% (v/v) heat-inactivated fetal calf serum (FCS) and 50 mg ml^{-1} gentamicin, in a humidified atmosphere at 5% CO_2 and 37 °C in 75 cm^2 flasks.[20] After reaching a ~70% confluence, the Caco-2 cells were sub-cultured, after rinsing with phosphate buffered saline (PBS), using trypsin (Gibco, Paisley, UK). Only cells within passage numbers 30–40 were used.

MTT assay

NR8383 cells. In this assay, the mitochondrial activity is determined photometrically by measuring the amount of MTT salt converted to insoluble formazan crystals by mitochondrial reductase enzymes. An NR8383 cell suspension was collected and centrifuged at 140*g* for 5 min before resuspending the cell pellet in a medium followed by counting and adjusting the cellular concentration to 2×10^5 cells per ml.[20] The cells were then seeded in a 96-well plate (50 μl per well) and the plate was kept in a 5% CO_2 incubator at 37 °C for 24 h. Next day, 50 μl of serial dilutions of Si NPs or Ge NPs were added to the cells to obtain the required final concentration range (0–100 μg ml^{-1}) of Si NPs or Ge NPs, and then the plates were incubated for 24 h. After 24 h, 5 μl of MTT (3-(4,5-dimethylthiazol-2-yl)-2,5-diphenyl tetrazolium bromide) solution in PBS (5 mg ml^{-1}) was added to each well and the plate was incubated for another 4 h. Then 100 μl of pure DMSO was added to each well to dissolve the formazan crystals. Now the absorption of each well was measured at 562 nm in a 96-well plate reader and the background absorption at 612 nm was subtracted. Mitochondrial metabolic activity for each concentration of Si NPs was expressed as % of the value of the corresponding negative control. F12-K medium without NPs and a medium with Triton-X (0.01%) were used as negative and positive controls respectively. Control experiments were done to exclude any possible reaction between MTT salt and Si NPs or Ge NPs by mixing test concentrations of the Si NPs or Ge NPs with the MTT reagent.

Caco-2 cells. The Caco-2 cells were plated at a concentration of 10^5 cells per ml in a 96-well plate (100 μl per well) and were incubated for 24 h.[20] Then the Si NPs or Ge NPs were added to the cells in a total volume of 100 μl at final exposure concentrations of 0–100 μg ml^{-1}. After this, the cells were incubated for another 24 h. After 24 h of exposure to the Si NPs or Ge NPs, 5 μl of MTT solution in PBS (5 mg ml^{-1}) was added to each well and incubated for 4 h. Then, the medium was removed and 100 μl of DMSO was added to dissolve the formed formazan crystals. The plates were put in the plate shaker for 5 min. The absorbance at both 562 nm and 612 nm was measured. The mitochondrial metabolic activity was expressed as the mean percentage of the negative control values (0 μg ml^{-1}). 0.01% Triton-X was used as the positive control and DMEM medium without Si NPs or Ge NPs was used as the negative control. Control tests were also done to exclude interfering reactions between the NPs and the MTT solution.

BrdU assay

NR8383 cells. The NR8383 cells were plated and exposed to Si NPs or Ge NPs (final exposure concentration 0–100 μg ml^{-1}) as described before. Cell proliferation was quantified using the colorimetric BrdU (5-bromo-2-deoxyuridine) assay (catalogue no. 647229001, Roche Diagnostics, Penzberg, Germany). BrdU acts as a structural analogue of thymidine and will be incorporated in newly synthesized DNA during cell replication and hence indicates cell proliferation.[21] After 24 h of incubation with NPs and BrdU, 100 μl of the BrdU labeling solution was added to each well followed by incubation for 4 h. The immunoassay was then performed as instructed by the manufacturer. A 0.01% Triton-X solution in F12-K medium was used as the positive control and F12-K medium without Si NPs or Ge NPs was used as the negative control.

Caco-2 cells. The Caco-2 cells were plated and exposed to Si NPs or Ge NPs as described before.[21] After incubation of the Caco-2 cells with the Si NPs or Ge NPs and BrdU for 24 h, the medium containing the Si NPs or Ge NPs and BrdU was removed, and the BrdU labeling solution was added to the wells and incubated for 4 h. Subsequently, the immunoassay was performed according to the protocol of the manufacturer. Results were expressed as the mean % of the negative control (0 μg ml^{-1}) values. 0.01% Triton-X in DMEM medium and DMEM medium without Si NPs or Ge NPs were used as positive and negative controls, respectively.

Induction of ROS from an isolated mitochondrial fraction from rat liver by DCFH-DA assay

An isolated mitochondrial fraction from rat liver tissue was prepared as described before.[20] The isolated mitochondrial fraction (3 mg pellet per ml in PBS) was plated in a 96-well plate (50 μl per well) and serial dilutions of Si NPs or Ge NPs and 5 μl of 20 mM DCFH-DA (2′,7′-dichlorofluorescein diacetate) probe (catalogue no. D6883/Sigma Aldrich Chemie BV) were added. The plate was incubated for 90 min at 37 °C in a humidified 5% CO_2 atmosphere. The plate was then measured at $\lambda_{ex} = 485$ nm and $\lambda_{em} = 538$ nm. Media without Si NPs or Ge NPs and with 75 μM DNP in DMSO were used as negative and positive controls, respectively. Results were expressed as % of the negative control (0 μg ml^{-1}).

Measurement of the mitochondrial membrane potential ($\Delta\Psi_m$)

The NR8383 and Caco-2 cells were plated as described above and exposed to serial test concentrations of NPs (0–100 μg ml^{-1}). The mitochondrial membrane potential ($\Delta\Psi_m$) was then measured using a commercially available kit from Invitrogen (MitoProbe™ Transition Pore Assay Kit; catalogue no. M34153) and the results were expressed as % of the negative control (0 μg ml^{-1}). A 100 μM solution of F12-K or DMEM medium containing ionomycin and a medium without NPs were used as positive and negative controls, respectively.

Measurement of the intracellular ATP content

The NR8383 and Caco-2 cells were seeded in a 96-well plate and exposed to different Si NPs or Ge NPs as mentioned before. After 24 h, the intracellular ATP content of each well was measured using a commercial ATP measuring kit (Sigma Aldrich, product no. FLASC) and results were expressed as % of the negative control (0 μg ml^{-1}). Cells exposed to a medium without NPs and to a medium with 75 mM 2,4-DNP (2,4-dinitrophenol) were used as negative and positive controls, respectively.

Measurement of cytoplasmic free Ca^{2+} content

The NR8383 and Caco-2 cells were plated and exposed to the serial test concentration range before measuring the cytoplasmic free calcium content using a commercially available kit from the Invitrogen (Fluo-4 Direct™ Calcium Assay Kit; catalogue no. F10472). Only F12-K or DMEM medium without NPs (0 μg ml^{-1}) was used as the negative control and the results were expressed as % of the negative control.

Measurement of intracellular ROS by DCFH-DA assay

NR8383 cells. The cell suspension was adjusted to 2×10^5 cells per ml and seeded in a 96-well plate (50 μl per well) in F12-K medium. 50 μl per well of serial dilutions of Si NPs or Ge NPs in F12-K medium were added to obtain the required final concentrations of Si NPs or Ge NPs. A final concentration of 10 mM H_2O_2 in F12-K medium was used as the positive control and F12-K medium without NPs as the negative control. After 6 h of exposure to the Si NPs or Ge NPs, 5 μl of a 20 mM solution of DCFH-DA were added to each well and the plates were incubated for another 18 h in a 5% CO_2 atmosphere at 37 °C. The fluorescence was then measured at $\lambda_{ex} = 485$ nm and $\lambda_{em} = 538$ nm. The fluorescence induction factor for each concentration of Si NPs or Ge NPs was then calculated by dividing the reading of each well with the average reading of the negative control (0 μg ml^{-1}) and expressed as %. Control experiments were performed by incubating the Si NPs or Ge NPs at their test concentrations with DCFH-DA in the absence of cells to check the possibility of a positive fluorescence reading caused by the reaction with NPs alone.

Caco-2 cells. The cells were suspended in DMEM medium to a concentration of 1×10^5 cells per ml after trypsinization and were plated in a 96-well plate (100 μl per well). After 24 h the cells were exposed to 100 μl per well of final concentrations of Si NPs or Ge NPs. Following another 6 h, 5 μl of a 20 mM solution of DCFH-DA in DMSO were added to each well. The plate was further incubated for 18 h before measurement of the fluorescence was carried out as described above. Control experiments were performed by incubating the Si NPs or Ge NPs at their test concentrations with DCFH-DA in the absence of cells to check the possibility of a positive fluorescence reading caused by the reaction with Si NPs or Ge NPs alone.

Measurement of TNF-α

The NR8383 and Caco-2 cells were seeded in a 96-well plate and exposed to different Si NPs or Ge NPs as mentioned before. After 24 h, the TNF-α content of each well was measured using a commercial TNF-α measuring kit (Invitrogen, catalogue no. KRC3011) and results were expressed as % of the negative control (0 μg ml^{-1}). A medium without NPs and a medium with 0.1 μg ml^{-1} lipopolysaccharide were used as negative and positive controls, respectively.

Measurement of caspase-3 activity

With prior plating and exposure of the NR8383 and Caco-2 cells to serial test concentrations of Si NPs or Ge NPs, the caspase-3 levels were measured using a commercially available kit from Sigma Aldrich Chemie BV (CASP3C). Results were expressed as % of the negative control (0 μg ml^{-1}).

Statistical analysis

The data were analyzed and plotted with the Origin Pro (Version 8.0) software. The results were presented as arithmetic mean ($n = 3$) ± standard error of mean (SEM).

Results and discussion

Si NPs and Ge NPs

The Si NPs and Ge NPs under investigation were obtained *via* four different synthetic approaches[10,18,21,49–52] in order to have a diverse mix of NPs with a wide range of surface properties. These NPs were all prepared from a Si or Ge core, which were subsequently surface-functionalized with different groups. The detailed characterization data including the abbreviations used for each of them are given in Table 1. This collection of Si NPs and Ge NPs could be classified into four groups based on their source: (1) Si NPs (1.6 ± 0.2 nm), synthesized from $SiCl_4$, with surface functionalizations of amine (Si(1.6) NP-NH_2), carboxylic acid (Si(1.6) NP-COOH) and azide (Si(1.6) NP-N_3).[10,18,21] These Si(1.6) NPs showed emission in the blue region upon excitation with UV light and their toxicity, or lack thereof, has been reported before;[20,21] these data are added for reference. The Si(1.6) NP-NH_2 were the only cytotoxic NPs within these three Si(1.6) NPs, whereas the Si(1.6) NP-COOH did not show any cytotoxicity up to 3 μg ml^{-1}.[20,21] The Si(1.6) NP-N_3 were toxic only at higher concentrations of >2 μg ml^{-1}. (2) Amine-terminated Si NPs (3.9 ± 1.3 nm) synthesized from *Zintl* salts ($NaSi_{1-x}M_x$, $x = 0.0, 0.05, 0.1, 0.15$; M = Mn, Fe), further on referred to as: Si(3.9) NP-NH_2. The synthetic route used allows the doping of these Si NPs with 1% manganese (Si_{Mn}(3.9) NP-NH_2), or 1% iron (Si_{Fe}(3.9) NP-NH_2). These three Si NPs were then also coated with dextran, referred to as Si(3.9) NP-NH_2-Dex, Si_{Mn}(3.9) NP-NH_2-Dex and Si_{Fe}(3.9) NP-NH_2-Dex. (3) Ge NPs (average size 5.5 ± 2.5 nm) with surfaces functionalized with polyethylene glycol (Ge NP-PEG) or *N*,*N*,*N*-trimethyl-3(1-propyne) ammonium iodide (Ge NP-TMPA) and Si NPs, surface-functionalized with PEG (Si NP-PEG).[52] (4) Si NPs (average size 2.5 ± 0.5 nm) functionalized with undecenylic acid (Si NP-UDA),[53] or linked *via* a dodecyl chain to a coating of poly(maleic anhydride)-based amphiphilic polymer (Si NP-Pol),[51] or silica (Si NP-Sil)[54] with average sizes of 17.8 ± 0.4 nm and 35 ± 5 nm, respectively. All the Si NPs and Ge NPs were well characterized with the dynamic light scattering (DLS) data on the dextran coated Si NP provided as ESI.† More extensive characterization of the NPs involved can be found elsewhere.[21,49,50] For the cluster of Si(1.6) NP-NH_2, Si(1.6) NP-COOH and Si(1.6) NP-N_3, the published reports[20,21] already provide us with knowledge on the toxicity which will be discussed in later sections. In the next group comprising Si(3.9) NP-NH_2, Si_{Mn}(3.9) NP-NH_2, Si_{Fe}(3.9) NP-NH_2 and dextran coated Si(3.9) NP-NH_2-Dex, Si_{Mn}(3.9) NP-NH_2-Dex, and Si_{Fe}(3.9) NP-NH_2-Dex, the comparison can be useful in several ways. As this group contained Si(3.9) NP-NH_2 bigger in size than Si(1.6)

Table 1 Data on different Si NPs and Ge NPs used in this study

NP	Surface functionalization	Dopant	Diameter (nm)	Abbreviations used	Graphical presentation
	$Si\text{-}C_3\text{-}NH_2$			$Si(1.6)\ NP\text{-}NH_3^+$ (ref. 10)	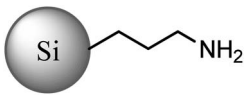
Si NP	$Si\text{-}C_{11}\text{-}N_3$	No	1.6 ± 0.2	$Si(1.6)\ NP\text{-}N_3$	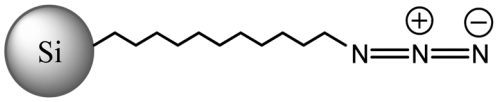
	$Si\text{-}C_4\text{-}COOH$			$Si(1.6)\ NP\text{-}COO^-$ (ref. 21)	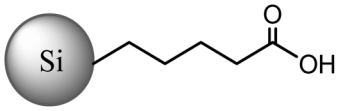
		No		$Si(3.9)\ NP\text{-}NH_3^+$ (ref. 50)	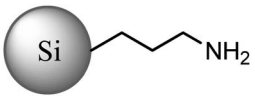
Si NP	$Si_M\text{-}C_3\text{-}NH_2$	Mn (1%)	3.9 ± 1.3	$Si_{Mn}(3.9)\ NP\text{-}NH_3^+$ (ref. 49)	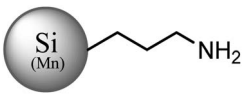
		Fe (1%)		$Si_{Fe}(3.9)\ NP\text{-}NH_3^+$	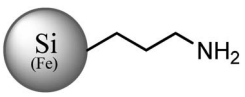
		No		$Si(3.9)\ NP\text{-}NH_2\text{-}Dex$	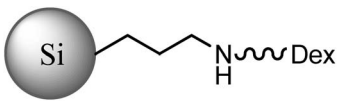
Si NP	$Si_M\text{-}C_3\text{-}NH_2\text{-}Dex$	Mn (1%)	3.9 ± 1.3	$Si_{Mn}(3.9)\ NP\text{-}NH_2\text{-}Dex$	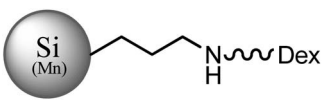
		Fe (1%)		$Si_{Fe}(3.9)\ NP\text{-}NH_2\text{-}Dex$	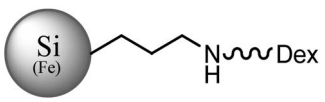
	Ge-PEG			Ge NP-PEG[52]	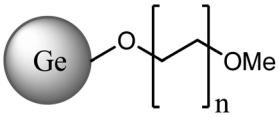
Ge NP		No			
	Ge-TMPA		5.5 ± 2.5	Ge NP-TMPA[52]	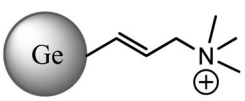
Si NP	Si-PEG			Si NP-PEG[52]	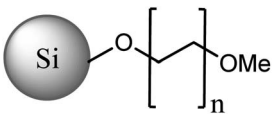
	Si-undecenylic acid		2.9 ± 0.5 (core)	Si NP-UDA[53]	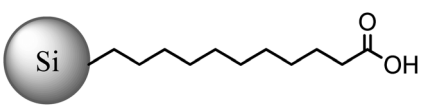
Si NP	$Si\text{-}C_{12}\text{-}Pol$		17.8 ± 0.4 (hydro-dynamic)	Si NP-Pol[51]	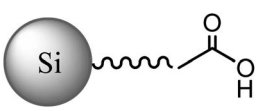
	$Si\text{-}C_{12}\text{-}Sil$		35 ± 5	Si NP-Sil	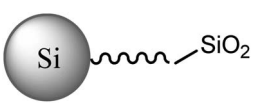

NP-NH_2, an indication of the influence of the size of NPs on their cytotoxicity can be obtained. The toxicity of the Mn- or Fe-doped Si(3.9) NPs can be compared to both Si(1.6) NP-NH_2 and Si(3.9) NP-NH_2 to find if the Mn or Fe dopants had any added toxic effects. This is important to learn, as the Si_{Mn}(3.9) NP-NH_2 and Si_{Fe}(3.9) NP-NH_2 have tremendous potential to be developed as bioimaging agents in the future and hence, an exacerbated toxicity is undesirable.

The dextran-coated Si NPs gave an interesting scope to compare the toxicity and find out whether the dextran coating can alleviate the toxicity. For the following group of Ge NP-PEG, Ge NP-TMPA and Si NP-PEG, a comparative investigation may reveal several important things. It has been claimed before that the balance between the hydrophilicity and hydrophobicity of NP surface coatings is important for the NP to exert cytotoxicity.[55,56] The Ge NP-PEG, Ge NP-TMPA, Si NP-Pol and Si NP-PEG differ in hydrophilicity and hence, an idea can be developed on the role of hydrophilicity in the toxic effects of Si NPs or Ge NPs. Furthermore, to investigate what effect the addition of PEG to the surface has, the toxicity of Si NP-PEG can be compared with Si(1.6) NP-NH_2 or Si(3.9) NP-NH_2. In the case of the group of Si NP-UDA and Si NP-Sil, it is relevant to investigate if toxicity is detected in spite of the fact that the Si NP-Sil had a non-toxic Si core, as silica is often reported to be toxic.[57,58]

MTT assay

The MTT assay measures the mitochondrial metabolic activity of the cells and this can be expressed as % cell viability of the negative control. In this study, the MTT assay was performed on both NR8383 and Caco-2 cells exposed to serial dilutions of Si NPs or Ge NPs (Fig. 1) for 24 h. From the results, it could be seen that only Si(3.9) NP-NH_2, Si_{Mn}(3.9) NP-NH_2, Si_{Fe}(3.9) NP-NH_2, Ge NP-TMPA and Si NP-Sil caused a dose-dependent reduction in cell viability, whereas the remaining Si NP/Ge NP did not show any toxicity within the tested concentration range (0–100 μg ml^{-1}). In the study by Bhattacharjee *et al.*,[20,21] among the Si(1.6) NP-NH_2, Si(1.6) NP-N_3 and Si(1.6) NP-COOH, only Si(1.6) NP-NH_2 was found to be toxic, followed by Si(1.6) NP-N_3, but only at comparatively high concentrations (>2 μg ml^{-1}).

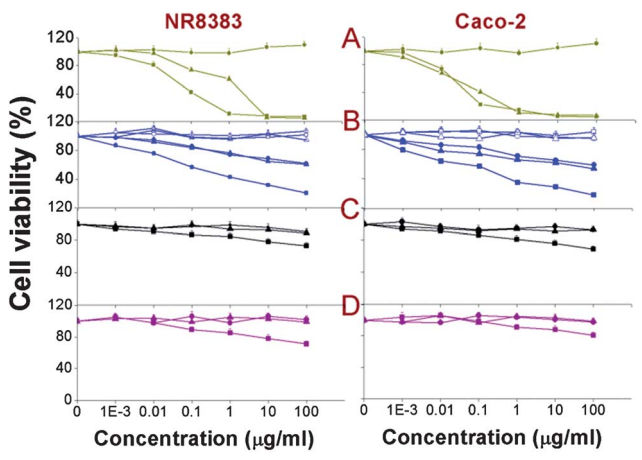

Fig. 1 MTT assay on NR8383 and Caco-2 cells after 24 h of exposure to: (A) Si(1.6) NP-NH_2 (■), Si(1.6) NP-N_3 (▲) and Si(1.6) NP-COOH (●); (B) Si_{Fe}(3.9) NP-NH_2 (■), Si(3.9) NP-NH_2 (▲), Si_{Mn}(3.9) NP-NH_2 (●), Si_{Fe}(3.9) NP-NH_2-Dex (□), Si(3.9) NP-NH_2-Dex (Λ) and Si_{Mn}(3.9) NP-NH_2-Dex (○); (C) Ge NP-TMPA (■), Ge NP-PEG (▲) and Si NP-PEG (●); (D) Si NP-Sil (■), Si NP-UDA (▲) and Si NP-Pol (●). Results are shown as mean ± standard error of mean (SEM) (n = 3).

While the toxicity of amine-terminated NPs is thus in line with previous observations, it is noteworthy that the addition of Mn doping did not yield any increased toxicity of Si_{Mn}(3.9) NP-NH_2 in comparison to Si(3.9) NP-NH_2. Such an increased toxicity upon doping was, however, observed for the iron-doped Si_{Fe}(3.9) NP, which may be attributed to the leaching out of Fe ions from the Si NPs core to the cellular environment or to the NPs surfaces, being responsible for the concomitant increase in overall toxicity. Perhaps the most relevant finding of this test was that coating the NP with PEG or dextran reduced the toxicity to nearly nil, even if the NP was doped with Fe or Mn. Apparently, the coating effectively blocked any leaching out in the case of Fe-doped Si NP and/or removed any toxicity of the remaining amine-groups or surfaced Fe ions 'hidden' under the polymeric coating. The EC_{50} values of all the NPs measured by the MTT assay are given in Table 2 for comparison.

BrdU assay

5-Bromo-2-deoxyuridine (BrdU) is a structural analogue of the thymidine base of DNA and gets incorporated within the strands of the DNA of proliferating cells and the amount of incorporated BrdU can then be measured spectrophotometrically.[59] As an adjunct to the MTT assay, which gives an idea on the effect on mitochondrial metabolic activity, the BrdU assay displays a DNA-based degree of continuing cell divisions, with the results presented as % of the negative control. The results obtained after 24 h of exposure of NR8383 and Caco-2 cells towards different Si NPs and Ge NPs are shown in Fig. 2 and the EC_{50} values are given in Table 2. From Fig. 2, it can be seen that apart from the amine-terminated Si(3.9) NP-NH_2, Si_{Mn}(3.9) NP-NH_2, Si_{Fe}(3.9) NP-NH_2 and Ge NP-TMPA, only Si NP-Sil were slightly cytotoxic, which matched well with the MTT assay data. The Si_{Mn}(3.9) NP-NH_2 did not show any added toxicity over Si(3.9) NP-NH_2, which encourages their further development as imaging agents.

The Si_{Fe}(3.9) NP-NH_2 again showed enhanced toxicity compared to the Si(3.9) NP-NH_2, which – as discussed with the MTT assay – can be an effect of the leaching Fe^{3+} ions from the core to the cellular environment or NP surfaces. In line with what was observed in the MTT assay, the dextran coating curbed the toxicity of not only Si_{Fe}(3.9) NP-NH_2 but also Si(3.9) NP-NH_2 and Si_{Mn}(3.9) NP-NH_2. The slight toxicity of Si NP-Sil can be attributed to the silica shell of these NPs. All the other Si NPs/Ge NPs were found to be non-toxic. In contrast to the positively charged NPs, the –OH or –COOH terminated Si NPs/Ge NPs did not show any effect on cell proliferation.[60] A possible reason behind less cytotoxicity is the comparatively reduced cellular uptake of anionic NPs compared to the cationic NPs. Various groups have observed such surface charge-dependent cellular uptake[59,60] and this phenomenon could also affect the toxicity of an NP and the role of surface properties in it.

Table 2 The EC_{50} values (μg ml^{-1}) for different Si NPs/Ge NPs obtained for the various endpoints reported in this article

		Si(1.6) NP-NH_2		Si(1.6) NP-N_3		Si(3.9) NP-NH_2		Si_{Mn}(3.9) NP-NH_2		Si_{Fe}(3.9) NP-NH_2		Ge NP-TMPA		Si NP-Sil	
Experiment	Fig.	NR8383	Caco-2	NR8383	Caco-2	NR8383	Caco-2	NR8383	Caco-2	NR8383	Caco-2	NR8383	Caco-2	NR8383	Caco-2
MTT	1	0.012 (ref. 20)	0.014 (ref. 21)	0.27 (ref. 20)	0.31 (ref. 21)	0.38	0.16	0.4	0.17	0.07	0.03	0.17	0.16	0.12	0.58
BrdU	2	0.02	0.011 (ref. 21)	0.26	0.28 (ref. 21)	0.15	0.12	0.16	0.14	0.08	0.05	0.22	0.21	0.18	0.37
Ψ_m	4	0.02	0.017	0.18	0.31	0.19	0.21	0.18	0.22	0.09	0.08	0.17	0.22	0.23	0.41
ATP	5	0.01	0.02	0.11	0.14	0.16	0.15	0.17	0.16	0.04	0.06	0.19	0.2	0.33	0.45
Cytoplasmic free Ca^{2+}	6	0.05	0.04	0.19	0.17	0.18	0.21	0.13	0.18	0.08	0.07	0.15	0.27	0.28	0.39
ROS (DCFH-DA)	7	0.022 (ref. 20)	0.018 (ref. 20)	0.17 (ref. 20)	0.31 (ref. 20)	0.21	0.22	0.2	0.23	0.09	0.08	0.18	0.19	0.29	0.34
TNF-α	8	0.1	0.2	0.18	0.28	0.18	0.19	0.22	0.21	0.08	0.11	0.19	0.21	0.33	0.39
Caspase-3	9	0.11	0.24	0.21	0.26	0.16	0.24	0.18	0.23	0.09	0.15	0.22	0.18	0.27	0.48
DCFH-DA (isolated mitochondrial fraction)	3	0.08 (ref. 20)		1.05 (ref. 20)		0.28		0.29		0.12		0.11		0.34	

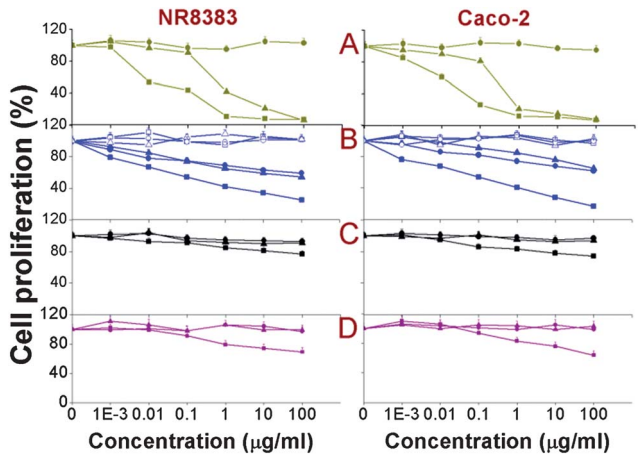

Fig. 2 BrdU assay on NR8383 and Caco-2 cells after 24 h of exposure to: (A) Si(1.6) NP-NH_2 (■), Si(1.6) NP-N_3 (▲) and Si(1.6) NP-COOH (●); (B) Si_{Fe}(3.9) NP-NH_2 (■), Si(3.9) NP-NH_2 (▲), Si_{Mn}(3.9) NP-NH_2 (●), Si_{Fe}(3.9) NP-NH_2-Dex (□), Si(3.9) NP-NH_2-Dex (Δ) and Si_{Mn}(3.9) NP-NH_2-Dex (○); (C) Ge NP-TMPA (■), Ge NP-PEG (▲) and Si NP-PEG (●); (D) Si NP-Sil (■), Si NP-UDA (▲) and Si NP-Pol (●). Results are shown as mean ± SEM ($n = 3$).

Induction of reactive oxygen species (ROS) from an isolated rat liver mitochondrial fraction by DCFH-DA assay

The mitochondrial fraction of liver tissue from a Wistar rat was prepared as reported before,[20] and these isolated mitochondria were incubated with serial dilutions of Si NPs and Ge NPs. DCFH-DA was used for the detection of reactive oxygen species (ROS). DCFH-DA is cleaved by nonspecific intramitochondrial esterases[61] to form DCFH. DCFH is further oxidized by ROS to form the fluorescent compound DCF (2′,7′-dichlorofluorescein), which was then measured ($\lambda_{ex} = 485$ nm; $\lambda_{em} = 538$ nm); the results are shown in Fig. 3 and the EC_{50} values are given in Table 2.

From our data, it is clear that only the cationic Si(3.9) NP-NH_2, Si_{Mn}(3.9) NP-NH_2, Si_{Fe}(3.9) NP-NH_2, Ge NP-TMPA and the hydroxyl-capped Si NP-Sil induced ROS production upon incubation with the isolated mitochondrial fraction. PEG-terminated Ge and Si NPs displayed no discernible ROS production. The ROS production induced by all the Si(3.9) NP-NH_2, Si_{Mn}(3.9) NP-NH_2 and Si_{Fe}(3.9) NP-NH_2 was decreased to almost none by the covalently bound dextran coating. How cationic NPs induce enhanced ROS production when incubated with isolated mitochondria is not fully understood, although as hypothesized for the outer cell membrane, electrostatic interactions between the negative lipid bilayer membranes and positive NPs may be a cause. Such an interaction between mitochondria and especially cationic polystyrene NPs has been noted before,[44] although to the best of our knowledge this is one of the first cases where such an interaction between intracellular mitochondria and semiconductor quantum dots is shown.

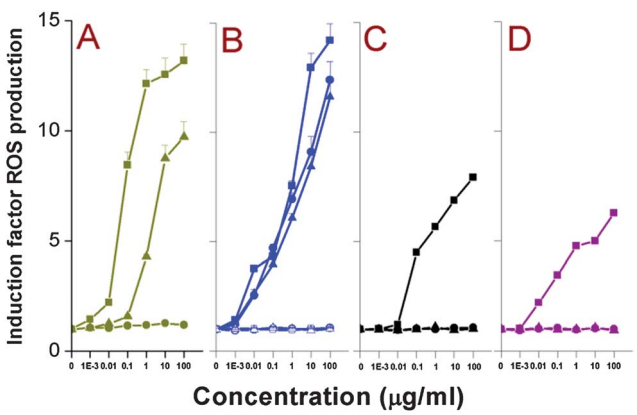

Fig. 3 DCFH-DA assay on an isolated rat liver mitochondrial fraction after 1.5 h of exposure to: (A) Si(1.6) NP-NH_2 (■), Si(1.6) NP-N_3 (▲) and Si(1.6) NP-COOH (●); (B) Si_{Fe}(3.9) NP-NH_2 (■), Si(3.9) NP-NH_2 (▲), Si_{Mn}(3.9) NP-NH_2 (●), Si_{Fe}(3.9) NP-NH_2-Dex (□), Si(3.9) NP-NH_2-Dex (Δ) and Si_{Mn}(3.9) NP-NH_2-Dex (○); (C) Ge NP-TMPA (■), Ge NP-PEG (▲) and Si NP-PEG (●); (D) Si NP-Sil (■), Si NP-UDA (▲) and Si NP-Pol (●). Results are shown as mean ± SEM ($n = 3$).

Measurement of the mitochondrial membrane potential ($\Delta\Psi_m$)

The change of the mitochondrial membrane potential ($\Delta\Psi_m$) can be an important parameter in understanding the mechanism of toxicity of NPs. A change in $\Delta\Psi_m$ indirectly shows the alteration in the mitochondrial membrane permeability, and might cause disruption of the electron transport chain (ETC). This may subsequently result in a decrease in ATP production and an induction of ROS production. The $\Delta\Psi_m$ in both the NR8383 and Caco-2 cell lines was measured after 24 h of exposure to different Si NPs and Ge NPs, and the results along with the corresponding EC_{50} values are shown in Fig. 4 and Table 2, respectively. Only exposure of the cells to the cationic amine-terminated NPs as well as to the Si NP-Sil resulted in a decrease in the $\Delta\Psi_m$ in contrast to exposure of the cells to anionic or PEG-terminated Si NPs and Ge NPs. Interestingly, a dextran coating over the Si(3.9) NP-NH_2, Si_{Mn}(3.9) NP-NH_2 and Si_{Fe}(3.9) NP-NH_2 minimizes also the effects on $\Delta\Psi_m$.

Measurement of intracellular ATP production

To investigate more deeply the effects of the interaction of the different Si NPs and Ge NPs with mitochondrial membranes and the probable disruption of the ETC, the intracellular ATP content was measured. The results are shown in Fig. 5 and the EC_{50} values are given in Table 2. In line with the observations made before, only exposure to the cationic Si(1.6) NP-NH_2, Si(3.9) NP-NH_2, Si_{Mn}(3.9) NP-NH_2, Si_{Fe}(3.9) NP-NH_2, Ge NP-TMPA, apart from the Si(1.6) NP-N_3 and Si NP-Sil, resulted in a decrease in intracellular ATP production. This further strengthens our hypothesis that the interaction of cationic NPs with the outer layer of mitochondrial membranes disrupts the ETC, which then results in a decreased ATP production. Interestingly, depletion of ATP can be a contributing factor to the toxicity of the Si NPs or Ge NPs. In line with the MTT and the BrdU assay data, the dextran coating basically removed the toxicity of Si(3.9) NP-NH_2, Si_{Mn}(3.9) NP-NH_2 and Si_{Fe}(3.9) NP-NH_2. While similar findings have been reported for 60–300 nm polystyrene NPs[44] and polydisperse (6–20 nm) starch-coated Ag NPs,[62] this is the first report of the effect of NP with different surface charges on the cellular ATP production for NPs that are smaller than the critical diameter of 5.5 nm, which is required for efficient renal clearance.[18]

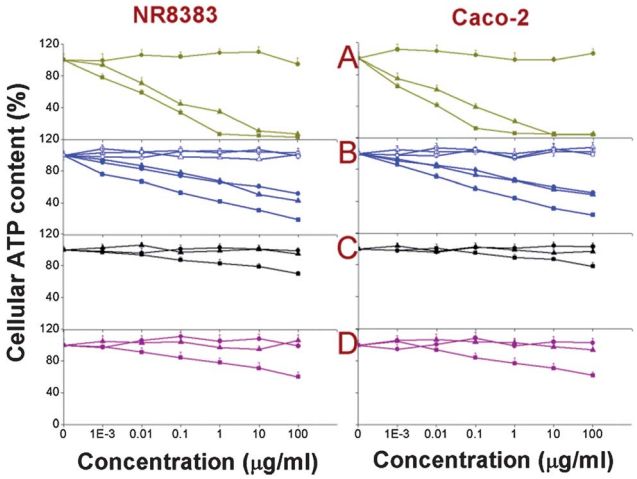

Fig. 5 Cellular ATP content in NR8383 and Caco-2 cells after 24 h of exposure to: (A) Si(1.6) NP-NH_2 (■), Si(1.6) NP-N_3 (▲) and Si(1.6) NP-COOH (●); (B) Si_{Fe}(3.9) NP-NH_2 (■), Si(3.9) NP-NH_2 (▲), Si_{Mn}(3.9) NP-NH_2 (●), Si_{Fe}(3.9) NP-NH_2-Dex (□), Si(3.9) NP-NH_2-Dex (△) and Si_{Mn}(3.9) NP-NH_2-Dex (○); (C) Ge NP-TMPA (■), Ge NP-PEG (▲) and Si NP-PEG (●); (D) Si NP-Sil (■), Si NP-UDA (▲) and Si NP-Pol (●). Results are shown as mean ± SEM (n = 3).

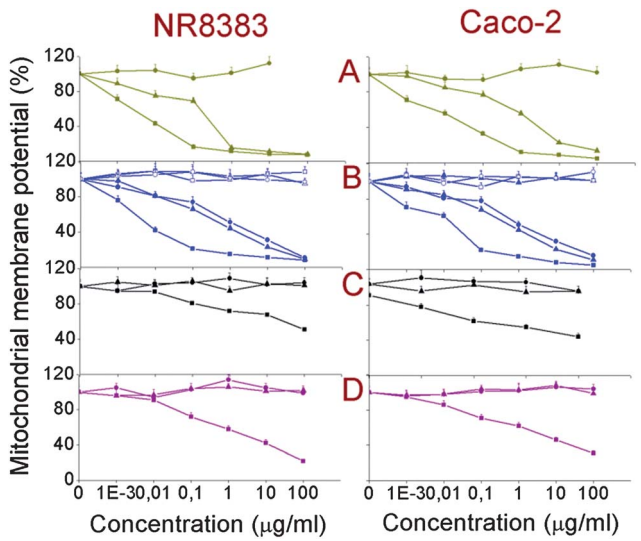

Fig. 4 Mitochondrial membrane potential (Ψ_m) in NR8383 and Caco-2 cells after 24 h of exposure to: (A) Si(1.6) NP-NH_2 (■), Si(1.6) NP-N_3 (▲) and Si(1.6) NP-COOH (●); (B) Si_{Fe}(3.9) NP-NH_2 (■), Si(3.9) NP-NH_2 (▲), Si_{Mn}(3.9) NP-NH_2 (●), Si_{Fe}(3.9) NP-NH_2-Dex (□), Si(3.9) NP-NH_2-Dex (△) and Si_{Mn}(3.9) NP-NH_2-Dex (○); (C) Ge NP-TMPA (■), Ge NP-PEG (▲) and Si NP-PEG (●); (D) Si NP-Sil (■), Si NP-UDA (▲) and Si NP-Pol (●). Results are shown as mean ± SEM (n = 3).

Measurement of cytoplasmic free Ca^{2+}

The cytoplasmic free calcium concentration is important in many aspects regarding the physiology of the cells. An increased free calcium content can not only disturb the ionic contents (K^+, Na^+, *etc.*) of the cellular cytoplasm, but can also trigger the apoptotic cascade that leads to programmed cell death. Here, the NR8383 and Caco-2 cells were exposed for 24 h to different test concentrations (0–100 μg ml^{-1}) of Si NPs and Ge NPs and cytoplasmic free Ca^{2+} levels were quantified. The results are shown in Fig. 6. The corresponding EC_{50} values are given in Table 2. The cationic NPs and Si NP-Sil showed a mild to moderate increase in cytoplasmic free calcium (order: Si_{Fe}(3.9) NP-NH_2 > Si(1.6) NP-NH_2 = Si_{Mn}(3.9) NP-NH_2 > Si(1.6) NP-N_3 > Ge NP-TMPA > Si NP-Sil), whereas no such increase could be seen for the anionic NPs or PEG-terminated and dextran-coated NPs.

Measurement of intracellular ROS production

In order to better understand our findings of especially cationic NPs causing an induction of ROS production in mitochondria along with causing a reduction in the cellular ATP

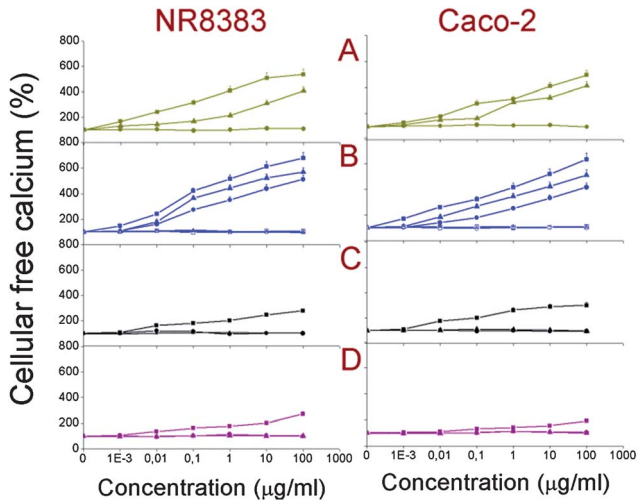

Fig. 6 Cellular free calcium in NR8383 and Caco-2 cells after 24 h of exposure to: (A) Si(1.6) NP-NH_2 (■), Si(1.6) NP-N_3 (▲) and Si(1.6) NP-COOH (●); (B) Si_{Fe}(3.9) NP-NH_2 (■), Si(3.9) NP-NH_2 (▲), Si_{Mn}(3.9) NP-NH_2 (●), Si_{Fe}(3.9) NP-NH_2-Dex (□), Si(3.9) NP-NH_2-Dex (△) and Si_{Mn}(3.9) NP-NH_2-Dex (○); (C) Ge NP-TMPA (■), Ge NP-PEG (▲) and Si NP-PEG (●); (D) Si NP-Sil (■), Si NP-UDA (▲) and Si NP-Pol (●). Results are shown as mean ± SEM (n = 3).

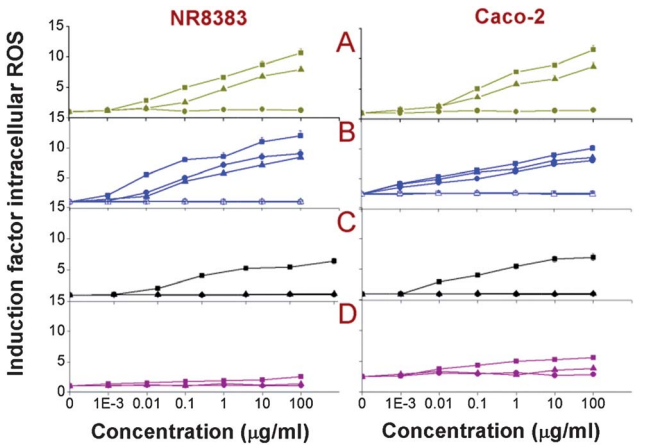

Fig. 7 DCFH-DA assay on NR8383 and Caco-2 cells after 24 h of exposure to: (A) Si(1.6) NP-NH_2 (■), Si(1.6) NP-N_3 (▲) and Si(1.6) NP-COOH (●); (B) Si_{Fe}(3.9) NP-NH_2 (■), Si(3.9) NP-NH_2 (▲), Si_{Mn}(3.9) NP-NH_2 (●), Si_{Fe}(3.9) NP-NH_2-Dex (□), Si(3.9) NP-NH_2-Dex (△) and Si_{Mn}(3.9) NP-NH_2-Dex (○); (C) Ge NP-TMPA (■), Ge NP-PEG (▲) and Si NP-PEG (●); (D) Si NP-Sil (■), Si NP-UDA (▲) and Si NP-Pol (●). Results are shown as mean ± SEM (n = 3).

concentration, the intracellular ROS concentration was measured. With data pointing towards possible damage caused by cationic Si NPs and Ge NPs of the mitochondrial membrane and decoupling of the electron transport chain, it is possible that the exaggerated production of ROS may cause oxidative stress. Several groups have hypothesized oxidative stress as the mechanism of NP cytotoxicity,[64–66] although the source of ROS is still not clear.

It is possible that damaged mitochondria with a compromised outer membrane integrity can be a source for the production of intracellular ROS. This would also suggest that intracellular oxidative stress is rather a secondary mechanism, which appears as a follow-up event to that of the mitochondrial interaction with cationic Si NPs or Ge NPs. The results of the DCFH-DA assay performed to measure the intracellular ROS production are shown in Fig. 7, with the EC_{50} values given in Table 2. In line with previous results, exposure of the cells to Si NP-Sil and the cationic Si(3.9) NP-NH_2, Si_{Mn}(3.9) NP-NH_2, Si_{Fe}(3.9) NP-NH_2 and Ge NP-TMPA resulted in an increase in intracellular ROS production. The negatively charged Si (1.6) NP-COOH, Si NP-UDA, and the dextran- or PEG-coated Si or Ge NPs did not induce ROS production.

Measurement of TNF-α

As a result of the oxidative stress and the injury inflicted by the different ROS radicals, an inflammatory response can be anticipated. The cytokine TNF-α (tumor necrosis factor-alpha or cachectin) is a pro-inflammatory biomarker that can be measured to identify an inflammatory response (see Fig. 8). Only the amine-terminated NPs (Si(1.6) NP-NH_2, Si(3.9) NP-NH_2, Si_{Mn}(3.9) NP-NH_2, Si_{Fe}(3.9) NP-NH_2, Ge NP-TMPA) and Si NP-Sil caused an induction in the production of TNF-α. The corresponding EC_{50} values are given in Table 2.

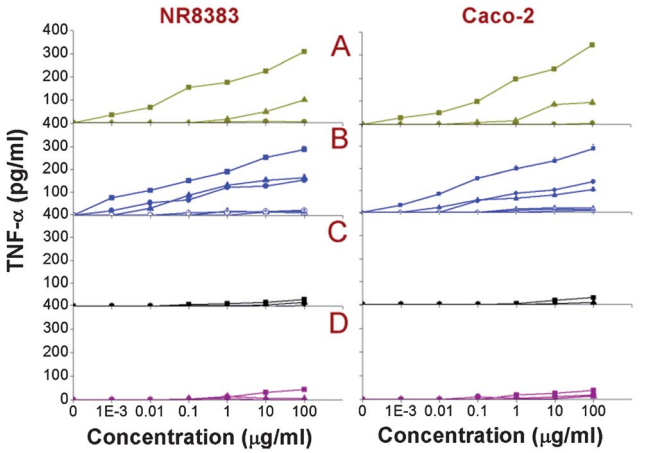

Fig. 8 Cellular TNF-α in NR8383 and Caco-2 cells after 24 h of exposure to: (A) Si(1.6) NP-NH_2 (■), Si(1.6) NP-N_3 (▲) and Si(1.6) NP-COOH (●); (B) Si_{Fe}(3.9) NP-NH_2 (■), Si(3.9) NP-NH_2 (▲), Si_{Mn}(3.9) NP-NH_2 (●), Si_{Fe}(3.9) NP-NH_2-Dex (□), Si(3.9) NP-NH_2-Dex (△) and Si_{Mn}(3.9) NP-NH_2-Dex (○); (C) Ge NP-TMPA (■), Ge NP-PEG (▲) and Si NP-PEG (●); (D) Si NP-Sil (■), Si NP-UDA (▲) and Si NP-Pol (●). Results are shown as mean ± SEM (n = 3).

Measurement of caspase-3 enzyme activity

The caspase-3 enzyme is an important biomarker for the apoptotic (self-programmed cell death) cascade. The caspase-3 activity was measured in NR8383 and Caco-2 cells after 24 h of exposure to the different Si NPs and Ge NPs and the results are shown in Fig. 9 with the EC_{50} values listed in Table 2. In line with the data obtained from the previously mentioned results in this paper, apart from the Si NP-Sil, only exposure to the cationic Si NPs/Ge NPs resulted in an increase of the caspase-3 activity. The observed order was Si_{Fe}(3.9) NP-NH_2 > Si(1.6) NP-NH_2 = Si_{Mn}(3.9) NP-NH_2 > Si(1.6) NP-N_3 > Si(3.9) NP-NH_2 > Ge NP-TMPA > Si NP-Sil, but the differences between these NPs were all relatively small. Characteristically, the Fe-containing

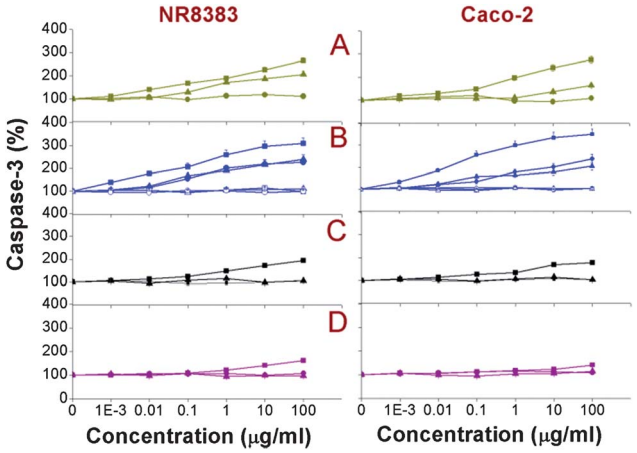

Fig. 9 Cellular caspase-3 activity in NR8383 and Caco-2 cells after 24 h of exposure to: (A) Si(1.6) NP-NH_2 (■), Si(1.6) NP-N_3 (▲) and Si(1.6) NP-COOH (●); (B) Si_{Fe}(3.9) NP-NH_2 (■), Si(3.9) NP-NH_2 (▲), Si_{Mn}(3.9) NP-NH_2 (●), Si_{Fe}(3.9) NP-NH_2-Dex (□), Si(3.9) NP-NH_2-Dex (△) and Si_{Mn}(3.9) NP-NH_2-Dex (○); (C) Ge NP-TMPA (■), Ge NP-PEG (▲) and Si NP-PEG (●); (D) Si NP-Sil (■), Si NP-UDA (▲) and Si NP-Pol (●). Results are shown as mean ± SEM (n = 3).

NPs yielded the highest caspase-3 induction. On the other hand, none of the anionic NPs, dextran-coated or PEG-ylated NPs showed any increase of the caspase-3 activity.

Analysis of toxicity tests

Upon comparison, it can be seen that, apart from Si NP-Sil, only cationic Si NPs/Ge NPs induced signs of cytotoxicity and effects on the nine endpoints evaluated in this study. The surface charge of an NP has been hypothesized to be an important factor in cytotoxicity of the NP.[37,63–65] Typically, positive NPs were found to be toxic whereas the anionic ones were not, which is in agreement with the current data. A detailed discussion on why positive surface charge-containing NPs are toxic in contrast to the negative NPs is beyond the scope of this article. However, it can be stated that positive NPs get electrostatically attracted towards the negative cell membrane,[66] thereby initiating cell membrane-bound receptor-mediated interactions and possibly also cell signaling cascades.[44] Within the group of amine-terminated Si NPs, the smaller Si(1.6) NP-NH_2, in line with previously reported relationships between the size and toxicity of NPs,[67–70] were found to be more toxic than the bigger Si(3.9) NP-NH_2. It should be mentioned here that it has been reported that it is the cationic charge carried by the amine groups in aqueous dispersions (as confirmed by their pK_a values[12]) rather than the amine group itself that contributes to the toxicity. For example, it has been reported that replacing the terminal amine groups with glucose moieties significantly reduced the toxicity of silicon nanowires in mouse stroma cells.[71] One possible explanation for this size-dependence of toxicity of NPs is that smaller NPs can have better access to different parts of the cells.

Additionally, smaller NPs have a more reactive surface area.[72] It was interesting to find that Mn-doped Si_{Mn}(3.9) NP-NH_2 did not show a higher cytotoxicity than either of the Si(3.9) NP-NH_2. This result is exciting in view of the potential of Mn-doped Si NP for bimodal bioimaging.[49] However, the Fe-doped Si_{Fe}(3.9) NP-NH_2 did show a higher cytotoxicity than Si(3.9) NP-NH_2. It was already reported that Fe has a tendency to leach out from the core of NPs as ions and cause toxicity.[73] The toxicity caused by the Fe^{3+} ions can be due to first their reduction to Fe^{2+} (by acidic lysosomes) and then reaction with mitochondrial and nuclear hydrogen peroxide to produce ROS *via* the Fenton reaction.[74,75] Remarkably, the toxicity could be diminished significantly when the Si_{Fe}(3.9) NP-NH_2 were coated by a covalently linked dextran coating. The dextran coating also abolished the toxicity of the other two toxic Si NPs: Si(3.9) NP-NH_2 and Si_{Mn}(3.9) NP-NH_2. This showed that a surface coating with a biocompatible material, like dextran, can strongly reduce the overall toxicity, and perhaps even turn the NP (nearly) non-toxic. The Si NP-Sil showed signs of toxicity although the toxicity was comparatively much lower. It has been reported that silica NPs are toxic,[57,58,76] and this can also be linked to the toxicity of Si NP-Sil. It was highly relevant to note that the carboxylic acid-terminated and hydroxyl-terminated Si NP-PEG, Ge NP-PEG, Si NP-UDA and Si NP-Pol did not show any toxicity within the tested concentration range. It has been reported that negative Si NPs were much less toxic compared to the positive ones.[20,21,34] This may be due to the fact that negative NPs get repelled by the negatively charged cell membranes, which hinders their cellular interactions. It has also been observed that the positive and negative NPs follow different endocytic uptake patterns in cells *via* activation of distinct groups of cell membrane receptors.[60,70,77,78] Interestingly, the interactions between lipid bilayer membranes and cationic NPs are of the same nature as the interactions between mitochondria and charge-bearing NPs. It is reported that cationic NPs cause an imbalance of the normal electrochemical gradient (80–130 mV)[79] across the outer mitochondrial membrane,[80] and thus yield an ionic imbalance and increased permeability. This can cause decoupling of ETC, an increase of intracellular ROS as well as a depletion of intracellular ATP production. Therefore we studied the effect of these NPs on the mitochondrial membrane potential and on the intracellular ATP production, with the results indicated in Fig. 4 and 5.

A silica coating on an intrinsically less or non-toxic Si-core would be of both chemical and toxicological interest investigating the effect of surface coating on toxicity of NPs as silica NPs have been reported to be toxic.[81] For such hybrid SiO_2/Si NPs, the presence of an organic coating is relevant, as this allows tuning of the hydrophilicity/hydrophobicity of the surfaces, which is reported to play an important role in the cellular interaction and uptake. Silica NPs have been reported to cause an induction of intracellular ROS,[82,83] an increase in the cytosolic free calcium concentration,[84] and an increased damage to the intra-nuclear DNA.[85] It is reported that cationic NPs (Si[21] and ZnO/CeO_2[34]) induced intracellular ROS production, and this matches with the current data. However, how these ROS are formed is yet unclear. It is possible that with their reactive nature, NPs can react with a wide variety of biomolecules inducing production of oxygen and nitrogen radicals or that they are the result of uncoupling of oxidative phosphorylation as such. A mitochondrial involvement in such an induction of ROS production seems to be a feasible explanation. It should also be mentioned here that the high

induction of ROS production following the exposure to the $Si_{Fe}(3.9)$ NP-NH_2 may be due to the leaching of Fe^{3+} ions from the core to the NPs surface or cellular environment. The results obtained from the TNF-α measurements point towards damage caused by the ROS, and show that the inflammatory behavior of the cells is a response to the toxic effects caused by the NPs. It is documented in the literature that especially cationic NPs (of different compositions, like lipids[86] or gelatin[87]) can cause an induction of TNF-α. Our data on the currently studied inorganic NPs are in line with the available literature.

Interestingly, an inverse relationship between the inflicted toxicity and size of the NPs can also be observed here, as the induction of TNF-α was found to be larger for the smaller Si(1.6) NP-NH_2 compared to the bigger Si(3.9) NP-NH_2, which is in line with the literature available for polystyrene[88] or metallic NPs.[63] The induction of TNF-α by the cationic Si NPs, found in the present study, also strengthened the idea that the inflammatory responses of the cells are caused by various radicals and ions. This can be pivotal in understanding the mechanism of cytotoxicity of different NPs.

Compilation of the available data and strategy to design more biocompatible Si NPs/Ge NPs

An analysis of the reported data in this article can not only lead to a better understanding of the mode of action underlying the cytotoxicity of these NPs, but may also help to develop smarter Si NPs or Ge NPs in future. In this article, we tried to show that the cell–NPs interaction can be evaluated on the basis of their surface properties, and hence it is of utmost importance that the surface chemistry of both the exposed cells and the NPs is known in detail. It has been reported that NPs interact preferentially with cell membrane-bound receptors.[12] In fact, by computational chemistry, the characteristics of these types of interactions between the cell membrane and NPs have recently been probed.[89] Besides that, the cationic surface charge has been recognized as an important factor in causing toxicity of NPs, and a surface charge-dependent cellular uptake pattern – with cationic NPs showing a higher cellular uptake compared to the anionic ones[12] – has also been observed. Interestingly, these two phenomena may be counteracting each other, as for targeted drug delivery it is important that the NPs combine a high cellular uptake with minimal toxicity. Hence, the finding that cationic NPs are usually more toxic can be a limiting factor for their possible applications in biological systems.

Recently, it has been shown that an alleviation of the toxicity of cationic NPs could be achieved by increasing the steric bulk around the positive charge of the NPs.[12] In the current study, the positive charge on the Ge NP-TMPA was also sterically hindered, and by simple comparison of EC_{50} values it can be stated that in equivalent amounts, the toxicity of these Ge NP-TMPA was smaller than that of the other amine-terminated NPs. Although this is just only the second example of such reduced toxicity, increasing the steric bulk around positive surface charges may be an interesting way of decreasing the toxicity of cationic NPs. More research is surely desired here to further delineate this phenomenon.

It is also important to have an idea of the surface functionalization of the NPs, as from our data it can be observed that a silica coating over a Si-core imparted toxic effects. Similarly, a coating with biocompatible dextran almost annulled the toxic effects of amine-terminated Si(3.9) NP-NH_2, $Si_{Mn}(3.9)$ NP-NH_2 and $Si_{Fe}(3.9)$ NP-NH_2. It is possible that the cells recognize the dextran moieties on the NPs surface and hence the cell–NPs interactions are immediately channeled in a different route, like activation of a different set of receptors. This is important to note, as it may provide some initial guidelines for functionalizing the surfaces of NPs which are targeted for biological applications. A review of literature on the toxicity of the coating materials as well as some control experiments with only the coating material can give initial predictions on the toxicity of NPs coated with the respective material.

Taken together, an indication towards surface reactivity-oriented interactions between the NPs and the cells can be obtained. It suggests analysis of the interactions between the cells and the NPs on the basis of chemical interactions possible between them. It is reported in the literature that different cell lines show dissimilar responses after being exposed to similar doses of the same NPs for the same time points,[44] which can be due to the fact that diverse cell lines express different cell membrane-bound receptors in varying quantities.[90] The interactions of NPs with cell membrane-bound receptors are quite specific and a variation in the amount of receptor protein expressed can also result in a variation of the exhibited toxicity. The battery of tests performed in the present study also enables us in getting a clear picture of the mechanism of toxicity of NPs.

A schematic diagram showing the proposed mechanism of cytotoxicity of cationic Si NPs/Ge NPs is given in Fig. 10. It seems that the mitochondria play a pivotal role in the entire mechanistic cascade of toxicity, where especially the cationic NPs, by creating damage to the normal physiology of the outer membrane of mitochondria, propel a series of events (like dissipation of ATP production, induction of ROS generation, cytoplasmic free calcium upload, oxidative stress, inflammatory response and finally triggering of apoptotic reactions) that ultimately sum up as the observed toxicity.

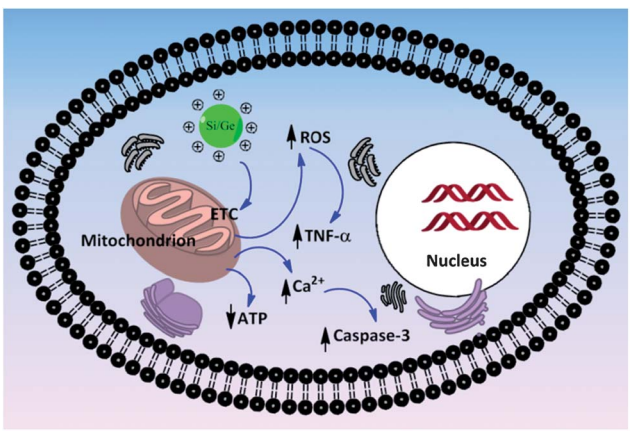

Fig. 10 Schematic diagram showing the proposed mechanism of cytotoxicity for cationic Si and Ge NPs.

In summary, in this article we have demonstrated by comparing the host of data obtained from a series of systematically varied Si NPs and Ge NPs that were subjected to a systematic set of toxicological *in vitro* experiments that the toxicity of Si NPs and Ge NPs is dominated by their surface chemistry. Whereas positively charged NPs displayed some toxicity, carboxylic acid-coated, dextran-coated and PEG-coated Si and Ge NPs displayed no toxicity in rat lung and human colon cell lines. Such surface-functionalized Si NPs or Ge NPs are of interest because of their intrinsic fluorescence, modifiable surfaces, minimally toxic cores and tunable doping with MRI active elements such as Mn and Fe. Given the suitable coating, these are thus highly attractive materials for biological and medical applications. Of course, it is not only looks (outside), but also size that matters: only smaller NPs (<5.5 nm) are typically effectively cleared *via* the kidneys.[17] Therefore, further research into Si or Ge NPs with a relatively small core, some bioinert, neutral coating, and possibly dopants for bimodal bioimaging seems highly attractive. In addition, if an effective renal clearance is undesired, Si NPs and Ge NPs do provide access to materials that combine a substantial larger size with minimal intrinsic toxicity. Finally, with this systematic set of toxicological investigations, a clear idea on the mechanism of cytotoxicity could be achieved, which puts intracellular mitochondria as one of the important targets for the toxicity of NPs.

Acknowledgements

The authors would like to thank Graduate school VLAG, the Wageningen UR strategic research program Bionanotechnology, QNano project nr: 262163, NIH (project: EB008576-01), DOE (DESC0002289), Natural Science and Engineering Council of Canada and Alberta Innovates and NSF Grant CMMI-0726943 for funding, and thank Prof. Angelique Louie (UC Davis) for useful discussions.

References

1 X. L. Luo, A. Morrin, A. J. Killard and M. R. Smyth, *Electroanalysis*, 2006, **18**, 319–326.
2 J. H. Lee, Y. M. Huh, Y. Jun, J. Seo, J. Jang, H. T. Song, S. Kim, E. J. Cho, H. G. Yoon, J. S. Suh and J. Cheon, *Nat. Med.*, 2007, **13**, 95–99.
3 L. Zhang, F. X. Gu, J. M. Chan, A. Z. Wang, R. S. Langer and O. C. Farokhzad, *Clin. Pharmacol. Ther.*, 2007, **83**, 761–769.
4 C. Buzea, I. Pacheco and K. Robbie, *Biointerphases*, 2007, **2**, MR17–MR71.
5 S. Lanone, F. Rogerieux, J. Geys, A. Dupont, E. Maillot-Marechal, J. Boczkowski, G. Lacroix and P. Hoet, *Part. Fibre Toxicol.*, 2009, **6**.
6 A. M. Iga, J. H. P. Robertson, M. C. Winslet and A. M. Seifalian, *J. Biomed. Biotechnol.*, 2007, 76087.
7 Y. Xing and J. H. Rao, *Cancer Biomarkers*, 2008, **4**, 307–319.
8 E. J. Anglin, L. Cheng, W. R. Freeman and M. J. Sailor, *Adv. Drug Delivery Rev.*, 2008, **60**, 1266–1277.
9 J. Fan and P. K. Chu, *Small*, 2010, **6**, 2080–2098.
10 M. Rosso-Vasic, E. Spruijt, Z. Popovic, K. Overgaag, B. van Lagen, B. Grandidier, D. Vanmaekelbergh, D. Dominguez-Gutierrez, L. De Cola and H. Zuilhof, *J. Mater. Chem.*, 2009, **19**, 5926–5933.
11 T. Oku, T. Nakayama, M. Kuno, Y. Nozue, L. R. Wallenberg, K. Niihara and K. Suganuma, *Mater. Sci. Eng., B*, 2000, **74**, 242–247.
12 S. Bhattacharjee, D. Ershov, J. v. d. Gucht, G. M. Alink, I. M. C. M. Rietjens, H. Zuilhof and A. T. M. Marcelis, *Nanotoxicology*, 2013, **7**, 71–84.
13 S. Chandra, P. Das, S. Bag, D. Laha and P. Pramanik, *Nanoscale*, 2011, **3**, 1533–1540.
14 N. K. Hon, Z. Shaposhnik, E. D. Diebold, F. Tamanoi and B. Jalali, *J. Biomed. Mater. Res., Part A*, 2012, **100**, 3416–3421.
15 A. M. Derfus, W. C. W. Chan and S. N. Bhatia, *Nano Lett.*, 2004, **4**, 11–18.
16 J. F. Popplewell, S. J. King, J. P. Day, P. Ackrill, L. K. Fifield, R. G. Cresswell, M. L. Di Tada and K. Liu, *J. Inorg. Biochem.*, 1998, **69**, 177–180.
17 H. S. Choi, W. Liu, P. Misra, E. Tanaka, J. P. Zimmer, B. I. Ipe, M. G. Bawendi and J. V. Frangioni, *Nat. Biotechnol.*, 2007, **25**, 1165–1170.
18 M. Rosso-Vasic, E. Spruijt, B. van Lagen, L. De Cola and H. Zuilhof, *Small*, 2008, **4**, 1835–1841.
19 J. H. Warner, A. Hoshino, K. Yamamoto and R. D. Tilley, *Angew. Chem., Int. Ed.*, 2005, **44**, 4550–4554.
20 S. Bhattacharjee, L. H. J. de Haan, N. M. Evers, X. Jiang, A. T. M. Marcelis, H. Zuilhof, I. M. C. M. Rietjens and G. M. Alink, *Part. Fibre Toxicol.*, 2010, **7**, 25.
21 L. Ruizendaal, S. Bhattacharjee, K. Pournazari, M. Rosso-Vasic, L. H. J. de Haan, G. M. Alink, A. T. M. Marcelis and H. Zuilhof, *Nanotoxicology*, 2009, **3**, 339–347.
22 K.-Q. Peng, X. Wang, L. Li, X.-L. Wu and S.-T. Lee, *J. Am. Chem. Soc.*, 2010, **132**, 6872–6873.
23 A. Shiohara, S. Prabakar, A. Faramus, C.-Y. Hsu, P.-S. Lai, P. T. Northcote and R. D. Tilley, *Nanoscale*, 2011, **3**, 3364–3370.
24 A. Shiohara, S. Hanada, S. Prabakar, K. Fujioka, T. H. Lim, K. Yamamoto, P. T. Northcote and R. D. Tilley, *J. Am. Chem. Soc.*, 2009, **132**, 248–253.
25 S. Prabakar, A. Shiohara, S. Hanada, K. Fujioka, K. Yamamoto and R. D. Tilley, *Chem. Mater.*, 2009, **22**, 482–486.
26 F. Maier-Flaig, E. J. Henderson, S. Valouch, S. Klinkhammer, C. Kübel, G. A. Ozin and U. Lemmer, *Chem. Phys.*, 2012, **405**, 175–180.
27 R. Anthony and U. Kortshagen, *Phys. Rev. B: Condens. Matter Mater. Phys.*, 2009, **80**, 115407.
28 C.-Y. Liu, Z. C. Holman and U. R. Kortshagen, *Nano Lett.*, 2008, **9**, 449–452.
29 A. R. Stegner, R. N. Pereira, R. Lechner, K. Klein, H. Wiggers, M. Stutzmann and M. S. Brandt, *Phys. Rev. B: Condens. Matter Mater. Phys.*, 2009, **80**, 165326.
30 A. Gupta, M. T. Swihart and H. Wiggers, *Adv. Funct. Mater.*, 2009, **19**, 696–703.
31 F. Erogbogbo, K.-T. Yong, I. Roy, R. Hu, W.-C. Law, W. Zhao, H. Ding, F. Wu, R. Kumar, M. T. Swihart and P. N. Prasad, *ACS Nano*, 2010, **5**, 413–423.

32 K. Dohnalová, A. Fučíková, C. P. Umesh, J. Humpolíčková, J. M. J. Paulusse, J. Valenta, H. Zuilhof, M. Hof and T. Gregorkiewicz, *Small*, 2012, **8**, 3185–3191.
33 J. Wang, Y. Liu, F. Peng, C. Chen, Y. He, H. Ma, L. Cao and S. Sun, *Small*, 2012, **8**, 2430–2435.
34 A. Shiohara, S. Hanada, S. Prabakar, K. Fujioka, T. H. Lim, K. Yamamoto, P. T. Northcote and R. D. Tilley, *J. Am. Chem. Soc.*, 2009, **132**, 248–253.
35 A. Asati, S. Santra, C. Kaittanis and J. M. Perez, *ACS Nano*, 2010, **4**, 5321–5331.
36 N. M. Schaeublin, L. K. Braydich-Stolle, A. M. Schrand, J. M. Miller, J. Hutchison, J. J. Schlager and S. M. Hussain, *Nanoscale*, 2011, **3**, 410–420.
37 A. M. El Badawy, R. G. Silva, B. Morris, K. G. Scheckel, M. T. Suidan and T. M. Tolaymat, *Environ. Sci. Technol.*, 2010, **45**, 283–287.
38 N. Shirahata, *Phys. Chem. Chem. Phys.*, 2011, **13**, 7284–7294.
39 J. R. Siekierzycka, M. Rosso-Vasic, H. Zuilhof and A. M. Brouwer, *J. Phys. Chem. C*, 2011, **115**, 20888–20895.
40 N. H. Alsharif, C. E. M. Berger, S. S. Varanasi, Y. Chao, B. R. Horrocks and H. K. Datta, *Small*, 2009, **5**, 221–228.
41 A. M. Scherbart, J. Langer, A. Bushmelev, D. van Berlo, P. Haberzettl, F. J. van Schooten, A. M. Schmidt, C. R. Rose, R. P. F. Schins and C. Albrecht, *Part. Fibre Toxicol.*, 2011, **8**, 31.
42 A. Nel, T. Xia, L. Mädler and N. Li, *Science*, 2006, **311**, 622–627.
43 X. Zhu, J. Zhou and Z. Cai, *Mar. Pollut. Bull.*, 2011, **63**, 334–338.
44 T. Xia, M. Kovochich, M. Liong, J. I. Zink and A. E. Nel, *ACS Nano*, 2007, **2**, 85–96.
45 T. Xia, M. Kovochich, M. Liong, L. Mädler, B. Gilbert, H. Shi, J. I. Yeh, J. I. Zink and A. E. Nel, *ACS Nano*, 2008, **2**, 2121–2134.
46 C. Uboldi, D. Bonacchi, G. Lorenzi, M. I. Hermanns, C. Pohl, G. Baldi, R. E. Unger and C. J. Kirkpatrick, *Part. Fibre Toxicol.*, 2009, **6**, 18.
47 M. Simon, P. Barberet, M.-H. Delville, P. Moretto and H. Seznec, *Nanotoxicology*, 2011, **5**, 125–139.
48 T. Xia, M. Kovochich, J. Brant, M. Hotze, J. Sempf, T. Oberley, C. Sioutas, J. I. Yeh, M. R. Wiesner and A. E. Nel, *Nano Lett.*, 2006, **6**, 1794–1807.
49 X. Zhang, M. Brynda, R. D. Britt, E. C. Carroll, D. S. Larsen, A. Y. Louie and S. M. Kauzlarich, *J. Am. Chem. Soc.*, 2007, **129**, 10668–10669.
50 X. M. Zhang, D. Neiner, S. Z. Wang, A. Y. Louie and S. M. Kauzlarich, *Colloidal Quantum Dots for Biomedical Applications II*, 2007, vol. 6448, p. 44804.
51 C. M. Hessel, M. R. Rasch, J. L. Hueso, B. W. Goodfellow, V. A. Akhavan, P. Puvanakrishnan, J. W. Tunnel and B. A. Korgel, *Small*, 2010, **6**, 2026–2034.
52 A. S. Heintz, M. J. Fink and B. S. Mitchell, *Adv. Mater.*, 2007, **19**, 3984–3988.
53 R. J. Clark, M. K. M. Dang and J. G. C. Veinot, *Langmuir*, 2010, **26**, 15657–15664.
54 S. Regli, J. A. Kelly and J. G. C. Veinot, *Mater. Res. Soc. Symp. Proc.*, 2011, **1359**, 149–154.
55 Y. Hoshino, H. Koide, K. Furuya, W. W. Haberaecker, S.-H. Lee, T. Kodama, H. Kanazawa, N. Oku and K. J. Shea, *Proc. Natl. Acad. Sci. U. S. A.*, 2012, **109**, 33–38.
56 P. Rivera Gil, G. Oberdörster, A. Elder, V. Puntes and W. J. Parak, *ACS Nano*, 2010, **4**, 5527–5531.
57 W. Lin, Y.-w. Huang, X.-D. Zhou and Y. Ma, *Toxicol. Appl. Pharmacol.*, 2006, **217**, 252–259.
58 T. Yu, A. Malugin and H. Ghandehari, *ACS Nano*, 2011, **5**, 5717–5728.
59 B. R. Prasad, N. Nikolskaya, D. Connolly, T. J. Smith, S. J. Byrne, V. A. Gerard, Y. K. Gun'ko and Y. Rochev, *J. Nanobiotechnol.*, 2010, **8**, 7.
60 A. E. Nel, L. Madler, D. Velegol, T. Xia, E. M. V. Hoek, P. Somasundaran, F. Klaessig, V. Castranova and M. Thompson, *Nat. Mater.*, 2009, **8**, 543–557.
61 H. Tazawa, C. Fujita, K. Machida, H. Osada and Y. Ohta, *Arch. Biochem. Biophys.*, 2009, **481**, 59–64.
62 P. V. AshaRani, G. Low Kah Mun, M. P. Hande and S. Valiyaveettil, *ACS Nano*, 2008, **3**, 279–290.
63 A. M. Schrand, M. F. Rahman, S. M. Hussain, J. J. Schlager, D. A. Smith and A. F. Syed, *WIREs Nanomedicine and Nanobiotechnology*, 2010, **2**, 544–568.
64 S. Mura, H. Hillaireau, J. Nicolas, B. Le Droumaguet, C. Gueutin, S. Zanna, N. Tsapis and E. Fattal, *Int. J. Nanomed.*, 2011, **6**, 2591–2605.
65 S. Bhattacharjee, D. Ershov, M. A. Islam, A. M. Kämpfer, J. v. d. Gucht, G. M. Alink, A. T. M. Marcelis, H. Zuilhof and I. M. C. M. Rietjens, *Nanotoxicology*, 2013, in press.
66 A. Verma and F. Stellacci, *Small*, 2010, **6**, 12–21.
67 Y. Pan, S. Neuss, A. Leifert, M. Fischler, F. Wen, U. Simon, G. Schmid, W. Brandau and W. Jahnen-Dechent, *Small*, 2007, **3**, 1941–1949.
68 B. M. Prabhu, S. F. Ali, R. C. Murdock, S. M. Hussain and M. Srivatsan, *Nanotoxicology*, 2010, **4**, 150–160.
69 Y.-S. Lin and C. L. Haynes, *J. Am. Chem. Soc.*, 2010, **132**, 4834–4842.
70 S. Bhattacharjee, D. Ershov, K. Fytianos, J. v. d. Gucht, G. M. Alink, I. M. C. M. Rietjens, A. T. M. Marcelis and H. Zuilhof, *Part. Fibre Toxicol.*, 2012, **9**, 11.
71 K. Jiang, D. Fan, Y. Belabassi, G. Akkaraju, J.-L. Montchamp and J. L. Coffer, *ACS Appl. Mater. Interfaces*, 2008, **1**, 266–269.
72 M. Auffan, J. Rose, J.-Y. Bottero, G. V. Lowry, J.-P. Jolivet and M. R. Wiesner, *Nat. Nanotechnol.*, 2009, **4**, 634–641.
73 H. Bouwmeester, J. Poortman, R. J. Peters, E. Wijma, E. Kramer, S. Makama, K. Puspitaninganindita, H. J. P. Marvin, A. A. C. M. Peijnenburg and P. J. M. Hendriksen, *ACS Nano*, 2011, **5**, 4091–4103.
74 M. A. Voinov, J. O. S. Pagán, E. Morrison, T. I. Smirnova and A. I. Smirnov, *J. Am. Chem. Soc.*, 2010, **133**, 35–41.
75 N. Singh, G. J. Jenkins, R. Asadi and S. H. Doak, *Nano Rev*, 2010, **1**, 5358.
76 Y. Jin, S. Kannan, M. Wu and J. X. Zhao, *Chem. Res. Toxicol.*, 2007, **20**, 1126–1133.
77 I. Lynch, A. Salvati and K. A. Dawson, *Nat. Nanotechnol.*, 2009, **4**, 546–547.
78 R. Vácha, F. J. Martinez-Veracoechea and D. Frenkel, *Nano Lett.*, 2011, **11**, 5391–5395.

79 D. Kleiner and E. Fitzke, *Biochim. Biophys. Acta, Biomembr.*, 1981, **641**, 138–147.
80 C. M. Goodman, C. D. McCusker, T. Yilmaz and V. M. Rotello, *Bioconjugate Chem.*, 2004, **15**, 897–900.
81 P. Ariano, P. Zamburlin, A. Gilardino, R. Mortera, B. Onida, M. Tomatis, M. Ghiazza, B. Fubini and D. Lovisolo, *Small*, 2011, **7**, 766–774.
82 D. Napierska, L. C. J. Thomassen, D. Lison, J. A. Martens and P. H. Hoet, *Part. Fibre Toxicol.*, 2010, **7**, 39.
83 R. K. Merchant, M. W. Peterson and G. W. Hunninghake, *J. Appl. Physiol.*, 1990, **68**, 1354–1359.
84 J. Chen, L. C. Armstrong, S. J. Liu, J. E. Gerriets and J. A. Last, *Toxicol. Appl. Pharmacol.*, 1991, **111**, 211–220.
85 R. P. F. Schins, R. Duffin, D. Hohr, A. M. Knaapen, T. M. Shi, C. Weishaupt, V. Stone, K. Donaldson and P. J. A. Borm, *Chem. Res. Toxicol.*, 2002, **15**, 1166–1173.
86 R. Kedmi, N. Ben-Arie and D. Peer, *Biomaterials*, 2010, **31**, 6867–6875.
87 K. Zwiorek, C. Bourquin, J. Battiany, G. Winter, S. Endres, G. Hartmann and C. Coester, *Pharm. Res.*, 2008, **25**, 551–562.
88 Y. Liu, W. Li, F. Lao, Y. Liu, L. Wang, R. Bai, Y. Zhao and C. Chen, *Biomaterials*, 2011, **32**, 8291–8303.
89 S. Zhang, J. Li, G. Lykotrafitis, G. Bao and S. Suresh, *Adv. Mater.*, 2009, **21**, 419–424.
90 M. Auffan, J. Rose, M. R. Wiesner and J.-Y. Bottero, *Environ. Pollut.*, 2009, **157**, 1127–1133.